Conformation of HIV-1 Envelope Governs Rhesus CD4 Usage and Simian-Human Immunodeficiency Virus Replication

Geraldine Vilmen,[a,b] Anna C. Smith,[a,b] Hector Cervera Benet,[c] Rajni Kant Shukla,[a,b] Ross C. Larue,[d] Alon Herschhorn,[c]
Amit Sharma[a,b]

aDepartment of Veterinary Biosciences, The Ohio State University, Columbus, Ohio, USA
bDepartment of Microbial Infection & Immunity, The Ohio State University, Columbus, Ohio, USA
cDivision of Infectious Diseases and International Medicine, Department of Medicine, University of Minnesota, Minneapolis, Minnesota, USA
dDepartment of Cancer Biology and Genetics, The Ohio State University, Columbus, Ohio, USA

ABSTRACT Infection of rhesus macaques with simian-human immunodeficiency viruses (SHIVs) is the preferred model system for vaccine development because SHIVs encode human immunodeficiency virus type 1 (HIV-1) envelope glycoproteins (Envs)—a key target of HIV-1 neutralizing antibodies. Since the goal of vaccines is to prevent new infections, SHIVs encoding circulating HIV-1 Env are desired as challenge viruses. Development of such biologically relevant SHIVs has been challenging, as they fail to infect rhesus macaques, mainly because most circulating HIV-1 Envs do not use rhesus CD4 (rhCD4) receptor for viral entry. Most primary HIV-1 Envs exist in a closed conformation and occasionally transit to a downstream, open conformation through an obligate intermediate conformation. Here, we provide genetic evidence that open Env conformations can overcome the rhCD4 entry barrier and increase replication of SHIVs in rhesus lymphocytes. Consistent with prior studies, we found that circulating HIV-1 Envs do not use rhCD4 efficiently for viral entry. However, by using HIV-1 Envs with single amino acid substitutions that alter their conformational state, we found that transitions to intermediate and open Env conformations allow usage of physiological levels of rhCD4 for viral entry. We engineered these single amino acid substitutions in the transmitted/founder HIV-1BG505 Envs encoded by SHIV-BG505 and found that open Env conformation enhances SHIV replication in rhesus lymphocytes. Lastly, CD4-mediated SHIV pulldown, sensitivity to soluble CD4, and fusogenicity assays indicated that open Env conformation promotes efficient rhCD4 binding and viral-host membrane fusion. These findings identify the conformational state of HIV-1 Env as a major determinant for rhCD4 usage, viral fusion, and SHIV replication.

IMPORTANCE Rhesus macaques are a critical animal model for preclinical testing of HIV-1 vaccine and prevention approaches. However, HIV-1 does not replicate in rhesus macaques, and thus, chimeric simian-human immunodeficiency viruses (SHIVs), which encode HIV-1 envelope glycoproteins (Envs), are used as surrogate challenge viruses to infect rhesus macaques for modeling HIV-1 infection. Development of SHIVs encoding Envs from clinically relevant, circulating HIV-1 variants has been extremely challenging, as such SHIVs replicate poorly, if at all, in rhesus lymphocytes. This is most probably because many circulating HIV-1 Envs do not use rhesus CD4 efficiently for viral entry. In this study, we identified conformational state of HIV-1 envelope as a key determinant for rhesus CD4 usage, viral-host membrane fusion, and SHIV replication in rhesus lymphocytes.

KEYWORDS HIV-1 envelope, CD4, rhesus macaque, SHIV, conformation, viral entry

The ability of viruses to efficiently utilize orthologous entry receptors determines which species can be infected, and this principle is often exploited for developing animal models of viral infection. Rhesus macaques serve as critical animal model for

preclinical human immunodeficiency virus type 1 (HIV-1) research. However, macaque models are limited by the fact that HIV-1 does not persistently infect macaques. Chimeric simian-human immunodeficiency viruses (SHIVs), constructed by replacing simian immunodeficiency virus (SIV) envelope glycoproteins (Envs) with that from HIV-1, have been developed as surrogates to study HIV-1 infection in rhesus macaques (1). Development of SHIVs has been a challenging process, mainly because most Envs from circulating HIV-1 variants do not use rhesus CD4 (rhCD4) efficiently for viral entry, and therefore, SHIVs replicate poorly in rhesus lymphocytes and do not establish persistent infection (2). Existing pathogenic SHIVs are a highly selected subset of viruses because they encode Envs from lab-adapted and chronic-stage HIV-1 variants, which can mediate entry using rhCD4. Moreover, to increase their pathogenicity, SHIVs generally require extensive adaptation to macaques (3–8), at least in part to optimize rhCD4-mediated entry (9). However, adaptation alters the antigenic features of Envs (10), limiting the translational utility of adapted SHIVs.

Binding of the metastable HIV-1 Env trimer to CD4 triggers a series of conformational changes in Env; i.e., the Env transitions from a functionally "closed" (state 1) to an "intermediate" (state 2) to an "open" (state 3) conformation (11–13). Unliganded Env trimers of most primary isolates only infrequently transit from closed to downstream, more open states (11, 14). The conformational dynamics of HIV-1 Envs can affect viral tropism by allowing adaptability to cells with different CD4 levels. For example, HIV-1 Envs that frequently sample state 2 and state 3 conformations can more efficiently infect cells that express low levels of human CD4 (huCD4) (15, 16). Importantly, the ability of HIV-1 Envs to utilize low levels of huCD4 positively correlates with their ability to utilize rhCD4 (17). Based on these insights, we hypothesized that open conformational states of HIV-1 Envs can overcome the rhCD4 entry barrier, which can, in turn, increase replication of SHIVs in rhesus lymphocytes. In this study, we generated HIV-1 Envs and SHIVs with single amino acid substitutions that alter Env conformational state. Our results show that SHIVs with open Env conformation bind and utilize rhCD4 efficiently and display higher viral fusion and replication in rhesus lymphocytes.

RESULTS

T/F and early-stage HIV-1 Envs do not use physiological levels of rhCD4 efficiently for viral entry. Envs of most circulating HIV-1 isolates from early stages of infection, including the transmitted/founder (T/F) variants, do not use rhCD4 efficiently for viral entry (17). To test our hypothesis that open Env conformations can overcome the rhCD4 entry barrier and mediate entry using physiological levels of rhCD4 expressed on rhesus lymphocytes, we first generated Cf2Th/syn CCR5 cells that stably express either low or high levels of rhCD4 (rhCD4$_{LOW}$ and rhCD4$_{HIGH}$). Importantly, we sorted and selected the rhCD4$_{LOW}$ cells such that their CD4 expression levels were representative of primary rhesus lymphocytes (Fig. 1). The cells were then infected with green fluorescent protein (GFP)-reporter HIV-1 pseudotyped with Envs that were obtained from HIV-1 isolates from acute/early stages of infection, including the T/F isolates (Table 1). As a control, Cf2Th/syn CCR5 cells expressing huCD4 were also infected and facilitated entry by all of these Envs (Fig. 2). In contrast to huCD4-mediated entry, rhCD4$_{LOW}$ cells did not facilitate efficient entry by seven out of eight Envs. Even with rhCD4$_{HIGH}$ cells, which express high levels of rhCD4, viral entry was much lower (~2.5- to 53-fold) than for huCD4. Only subtype D Env 191859 was able to gain entry into rhCD4$_{LOW}$ cells, but it was still ~1.7-fold lower than huCD4, highlighting that there are some rare primary Env that can inherently utilize rhCD4. As positive controls, two Envs from chronic-stage HIV-1 isolates (JR-FL and BaL) were tested and were able to gain entry using both huCD4 and rhCD4—consistent with the ability of Envs from lab-adapted and chronic-stage isolates to utilize rhCD4 for entry (17).

Transitions to intermediate and open Env conformations allow usage of rhCD4 for viral entry. Recent studies have suggested that Envs of most primary HIV-1 isolates exist in a closed conformation and only infrequently transit to downstream, more open conformations (11, 13, 18, 19). The ability of unliganded or CD4-bound Envs to transit
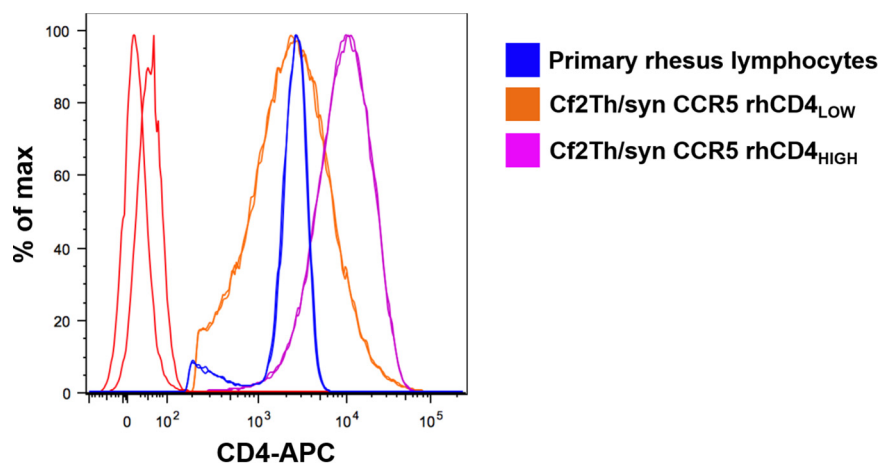
FIG 1 Expression levels of rhCD4 stably introduced into Cf2Th/syn CCR5 cells. Shown are expression levels of CD4 on primary rhesus macaque lymphocytes and rhCD4$_{LOW}$ and rhCD4$_{HIGH}$ Cf2Th/syn CCR5 cell lines as measured by flow cytometry using an APC-conjugated anti-CD4 antibody. The histograms represent the expression of CD4 on the cell surface. The data are representative of those from two independent experiments.

to downstream states can affect viral tropism by allowing adaptability to cells with different CD4 levels (15, 16). Thus, we sought to determine how the conformational states of HIV-1 Envs affect the ability to utilize rhCD4 for viral entry. We took advantage of the fact that single amino acid substitutions in the gp120 domain of HIV-1 Env trimer can alter its conformational state (15, 16). For example, L193A substitution in the V1/V2 loop of gp120 allows Envs to populate the state 2 conformation. I423A substitution in the $\beta20$-$\beta21$ element of gp120 allows Envs to populate the state 3 conformation. We engineered L193A and I423A substitutions in three different Envs representing a T/F (BG505.W6M.C2), an acute-stage clone (ZM53M.PB12), and a chronic-stage isolate (JR-FL). For the two early-stage Envs, I423A substitution mediated entry in rhCD4$_{LOW}$, rhCD4$_{HIGH}$, and huCD4 cells with similar efficiencies, whereas the L193A substitution displayed lower efficiency of entry in rhCD4$_{LOW}$ cells than in huCD4 and rhCD4$_{HIGH}$ cells (Fig. 3A and B). As controls, we used the related wild-type (WT) Envs that utilized huCD4 efficiently but did not gain efficient entry even in cells that express high levels of rhCD4. The chronic-stage JR-FL Env was able to gain entry using both huCD4 and rhCD4—independent of Env conformational state or rhCD4 expression levels (Fig. 3C). Similar patterns of rhCD4 usage were observed at different multiplicities of infection (MOIs), indicating that the ability of open Env conformations to use physiological levels of rhCD4 is independent of virus input (see Fig. S1 in the supplemental material). Thus, our results suggest that single amino acid substitutions in Env that promote transitions to intermediate and open conformations allow more efficient usage of physiological levels of rhCD4 for viral entry.

TABLE 1 Transmitted/founder and early-stage Env clones used in this study

Envelope clone	Subtype	Mode of natural transmission[a]	Source[b]	GenBank accession no.	Time postinfection (wks)
BG505.W6M.C2	A	M-C	PBMC	DQ208458	6
Q23.17	A	M-F	PBMC	AF004885	11
TRO.11	B	M-M	ccPBMC	AY835445	4
CAAN5342.A2	B	M-M	Plasma	AY835452	<12
Du422.1	C	M-F	ccPBMC	DQ411854	8
ZM53M.PB12	C	F-M	PBMC	AY423984	<12
QB857.110I.B3	D	M-F	PBMC	FJ866138	16
191859	D	M-F	Plasma	JX203064	Fiebig I

[a]M-C, mother to child; M-F, male to female; M-M, male to male; F-M, female to male.
[b]PBMC, Env cloned from uncultured PBMCs isolated directly from patient; ccPBMC, patient PBMCs (or virus from these PBMCs) underwent short-term coculture with PBMCs from HIV-1-negative donors to amplify virus before cloning; Plasma, Env cloned from virion RNA in plasma isolated directly from patient.
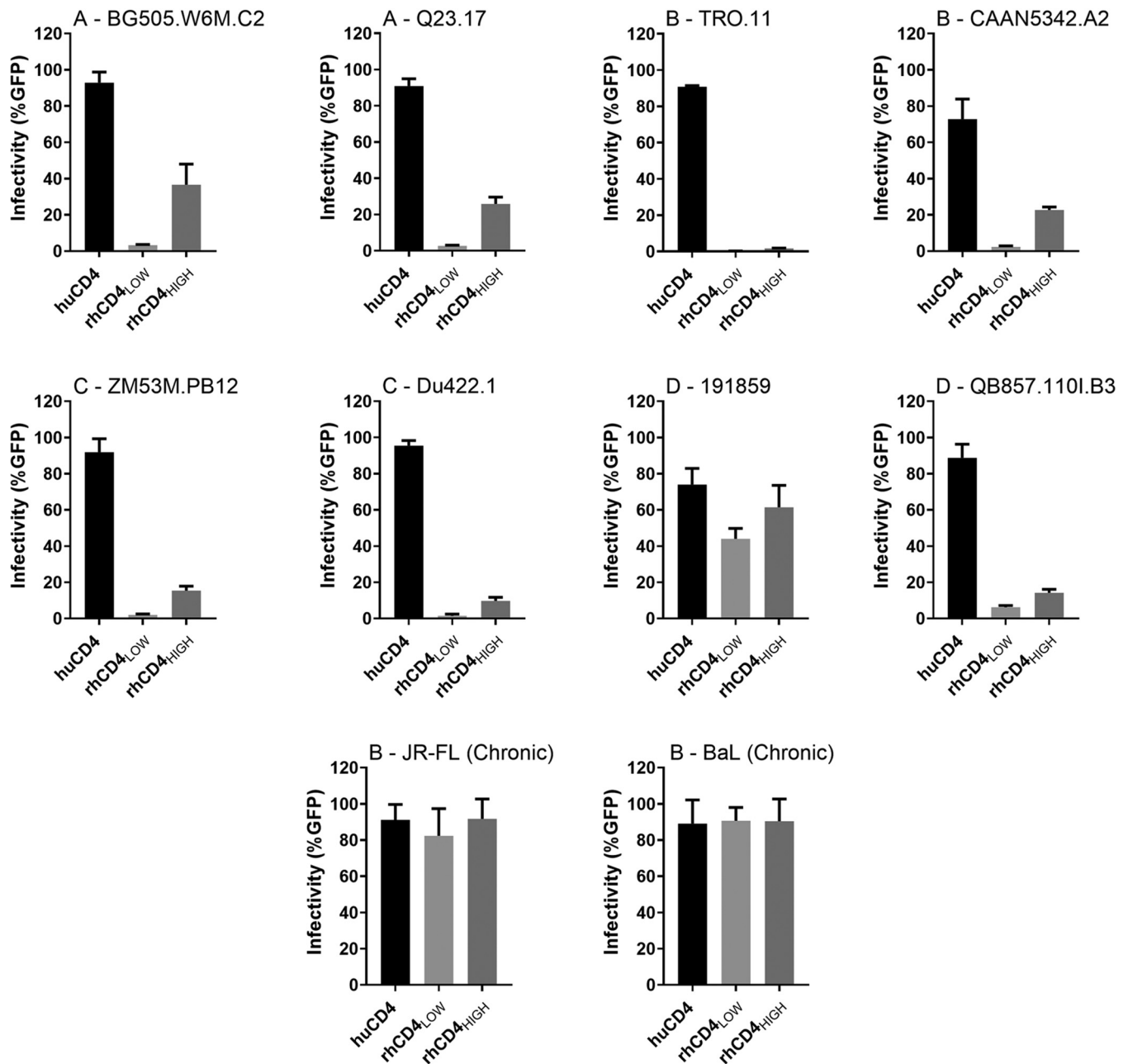
FIG 2 Ability of transmitted/founder and early-stage HIV-1 Envs to use physiological levels of rhCD4 for viral entry. Cf2Th/syn CCR5 cells expressing human or rhesus CD4 (indicated along the *x* axis) were infected with HIV-1$_{Q23\Delta EnvGFP}$ pseudotyped with indicated Env clones. Infection was measured by flow cytometry as percentage of GFP-positive cells 48 h postinfection. Graphs show percentage of infected cells for indicated Env at a multiplicity of infection of 1. Env clones are labeled at the top, with first letter indicating the subtype. Bars represent the averages from three independent experiments. Error bars represent standard deviations.

Open Env conformations promote replication of SHIV-BG505 in rhesus lymphocytes.

Next, we sought to determine whether improved rhCD4 usage by Envs that are in intermediate and open conformational states translate into enhanced replication of T/F SHIV in rhesus lymphocytes. For this purpose, we introduced the L193A or I423A substitution in the HIV-1$_{BG505}$ T/F Envs encoded by SHIV-BG505. Importantly, we also included SHIV-BG505 with A204E substitution in the C1 region of gp120 as a benchmark control for replication. The A204E adaptive mutation, previously identified through serial passage of primary HIV-1 Envs in immortalized macaque CD4+ T lymphocytes (20), was sufficient to mediate viral entry in rhCD4$_{LOW}$ cells at levels comparable to those in huCD4 cells (Fig. S2). More importantly, the A204E substitution induces
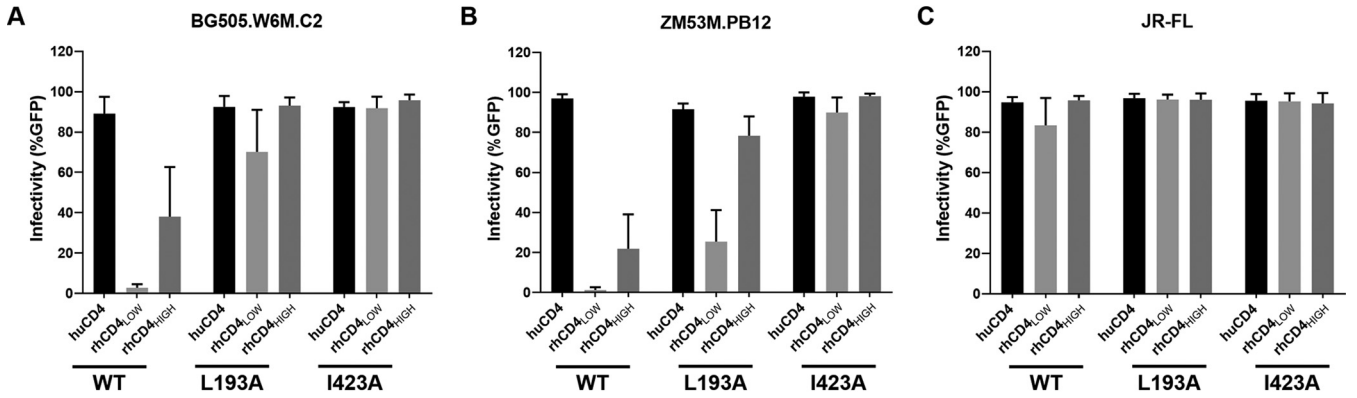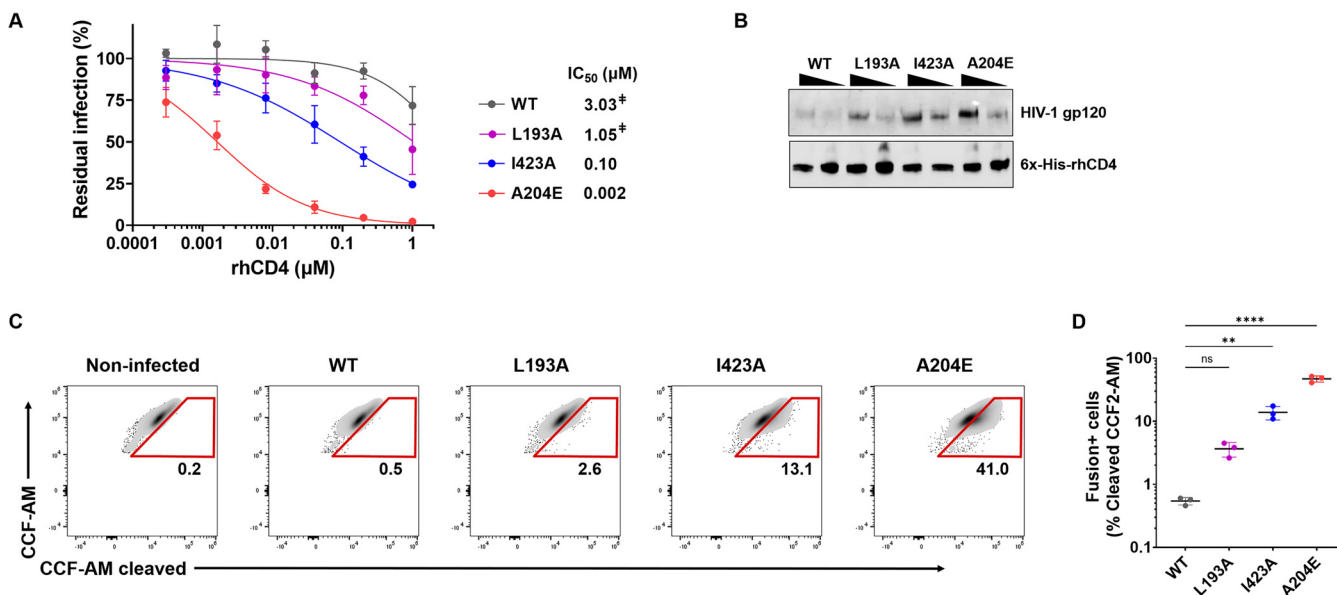
FIG 3 Effect of Env conformation on usage of rhCD4 for viral entry. Cf2Th/syn CCR5 cells expressing human or rhesus CD4 (indicated along the x axis) were infected with HIV-1$_{Q23\Delta EnvGFP}$ pseudotyped with BG505.W6M.C2 (A), ZM53M.PB12 (B), and JR-FL (C) Env clones. Infection was measured by flow cytometry as percentage of GFP-positive cells 48 h postinfection. Graphs show percentage of infected cells for wild-type (WT), L193A, and I423A Envs at a multiplicity of infection of 1. Bars represent the averages from three independent experiments. Error bars represent standard deviations.

conformational changes in the Envs that open up the Env trimers on the surface of virions (10), which likely explains its ability to utilize physiological levels of rhCD4. We measured the ability of these SHIVs to replicate in the immortalized rhesus macaque CD4$^+$ T lymphocytes (21). As expected, the replication of SHIV encoding wild-type Envs (WT SHIV), which do not utilize rhCD4 efficiently, declined over the 15-day time course, indicating that it does not replicate in rhesus cells (Fig. 4). SHIVs encoding I423A or A204E substitutions replicated to significantly higher levels over the 15-day time course than WT SHIV. Interestingly, SHIV L193A, which encodes Env with an intermediate open conformation that allows it to use rhCD4 better than the WT Envs (Fig. 3A), did not display significantly improved growth kinetics compared to WT SHIV. Based on these findings, we conclude that open Env conformations, such as those conferred by I423A and A204E mutations, promote replication of SHIV-BG505 in rhesus lymphocytes.

Open Env conformations promote CD4 binding and viral fusion. Finally, we examined whether open Env conformations promote SHIV replication by enhancing rhCD4 binding and viral fusion. We evaluated the effects of Env conformation on rhCD4 binding by two independent approaches. First, we performed neutralization assays to measure the ability of soluble rhCD4 to bind functional Env trimers on SHIVs
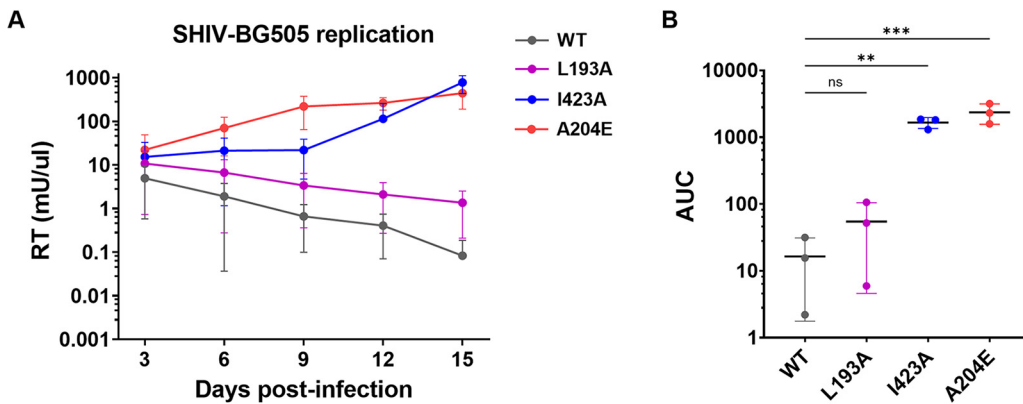
FIG 4 Effect of Env conformation on SHIV replication. (A) Replication kinetics of SHIV-BG505 variants in rhesus macaque 221 T lymphocytes over a 15-day time course. Reverse transcriptase (RT) activity in viral supernatants is plotted versus days postinfection. The key at the right of the graph indicates the identity of the Env variant (WT or indicated amino acid mutation) encoded by each SHIV. Each data point represents the average from three independent experiments, performed in duplicate. Error bars represent standard deviations. (B) Area under the curve (AUC) for indicated SHIV variants (x axis) determined from the replication curves shown in panel A. AUC values were compared to those for the SHIV-BG505 WT using one-way analysis of variance (ANOVA) followed by Dunnett's multiple-comparison test. ***, P = 0.0004; **, P = 0.004. ns, not significant.

FIG 5 Effect of Env conformation on rhCD4 binding and viral fusion. (A) Sensitivity of SHIV-BG505 to neutralization by soluble rhCD4. Neutralization curves of the indicated SHIV variants were generated by plotting percent residual infection (y axis) against rhCD4 concentration (x axis). Each data point represents the average from two independent experiments, performed in duplicate. Error bars represent standard deviations. The calculated $IC_{50}s$ are shown. Where IC_{50} values were above the highest tested concentration, the extrapolated concentration is indicated by a double dagger. (B) Binding of SHIV-BG505 to rhCD4. Western blot analysis for affinity pulldown of His-tagged rhCD4 was performed with increasing amounts (400 and 800 mU of RT) of indicated SHIV virions. Immunoblotting was performed using anti-HIV-1 gp120 and anti-6×His antibodies. (C) Representative flow cytometry plots indicating percent viral fusion. Fusion of indicated SHIV-BG505 variants with rhesus macaque 221 T lymphocytes was measured as percentage of cells with cleaved CCF2-AM substrate. The identity of the Env variant (WT or indicated amino acid mutation) encoded by each SHIV is indicated above the plots. (D) Graph of percent viral fusion for indicated SHIV variants (x axis). Data represent the averages from three independent experiments, with individual data points shown as circles. Error bars represent standard deviations. Percent viral fusion was compared to that for the SHIV-BG505 WT using one-way ANOVA followed by Dunnett's multiple-comparison test. ****, $P < 0.0001$; **, $P = 0.0024$.

and compete with receptor binding to inhibit viral entry. WT SHIV was least sensitive to rhCD4 inhibition, indicating that it does not efficiently bind rhCD4 and interfere with receptor binding (Fig. 5A). SHIV L193A and SHIV I423A, which are stabilized in state 2 and state 3 Env conformations, respectively, were ~3-fold and ~30-fold more sensitive to rhCD4 inhibition than WT SHIV, suggesting that progressive opening of the Envs increases rhCD4 binding. SHIV A204E was most sensitive (~1,500-fold) to rhCD4 inhibition, suggesting that it has the highest binding for rhCD4, likely attributable to "more open" conformation of its Env trimers. Similar neutralization trends, but with ~2- to 10-fold more potent inhibition, were observed with soluble huCD4, indicating that HIV-1 Envs encoded by these SHIVs bind huCD4 with higher affinity than rhCD4 (Fig. S3A). Second, we employed a qualitative affinity pulldown assay to determine the binding of rhCD4 to Envs expressed on infectious SHIVs. Virions bound to His-tagged rhCD4 were affinity precipitated and their Env levels were measured by immunoblotting. Consistent with the results of the neutralization assay, progressive opening of the Env resulted in more virions binding to rhCD4, with highest binding observed in the case of SHIV A204E (Fig. 5B). Similar binding patterns were also observed when pulldowns were performed with huCD4 (Fig. S3B). Lastly, we investigated how Env conformation affects fusion of SHIVs with rhesus lymphocytes using a SHIV fusion assay. WT SHIVs, which did not efficiently bind rhCD4, were not fusogenic with the target cells (Fig. 5C and D). SHIV L193A and SHIV I423A, which are stabilized in state 2 and state 3 Env conformations, respectively, were ~7-fold and ~25-fold more fusogenic than WT SHIV, suggesting that fusogenicity increases with progressive opening of the Envs. SHIV A204E was the most fusogenic, with ~87-fold-higher fusion than WT SHIV. Taken together, our results demonstrate that inducing open Env conformations, by introducing the I423A and A204E mutations, increases binding of Env to rhCD4 and subsequent SHIV-host membrane fusion.

DISCUSSION

Here, we provide first genetic evidence that conformational state of HIV-1 Envs governs rhCD4 usage. Using HIV-1 Envs with single amino acid substitutions that altered their conformational states, we demonstrated that transitions to intermediate and open Env conformations allow usage of physiological levels of rhCD4 for viral entry, which is otherwise a suboptimal receptor for entry. Moreover, by introducing these changes into the isogenic SHIV backbone, we found that open Env conformations promote rhCD4 binding, fusion-mediated cell entry, and replication in rhesus lymphocytes.

Thermodynamically, most primary HIV-1 Envs are in a high-free-energy, closed conformation. Single-molecule fluorescence resonance energy transfer studies have demonstrated that either spontaneously or upon CD4 binding, Env transitions from closed (state 1) to open (state 3) conformation through a functional intermediate (state 2) (11). Multiple amino acid residues restrain Env in state 1 and CD4 binding triggers Env transitions from state 1 to downstream, lower-energy states (15, 16, 22–25). For example, L193A and I423A substitutions release the state 1 restraints and stabilize Env in state 2 and state 3 conformations, respectively. Our findings of improved rhCD4 usage by Envs bearing L193A and I423A substitutions suggest that transitions to intermediate and open conformations advance HIV-1 Env on the entry pathway and likely facilitate Env engagement with a suboptimal rhCD4 receptor. Although Envs with L193A substitutions, which are in intermediate open conformations, utilized rhCD4 better than WT Env, SHIV encoding the L193A substitution did not display significantly improved viral fusion or replication. In contrast, SHIVs encoding Envs with I423A and A204E substitutions, which are in more open conformations, displayed significantly increased rhCD4 engagement, viral fusion, and replication. One possible explanation for the differences in growth kinetics of SHIVs encoding L193A and I423A substitutions could be the ~2- to 3-fold-lower infectivity of L193A Envs than I423A Envs. During spreading infection in rhesus lymphocytes, which involves multiple rounds of infection over a 15-day time course, the differences in absolute infectivity are likely amplified over time and are reflected in robust differences in viral growth kinetics. Overall, our results indicate that open Env conformations conferred by I423A and A204E mutations promote rhCD4 binding, viral fusion, and replication of SHIV in rhesus lymphocytes. Collectively, these findings suggest that modulating the conformational dynamics of viral Env by altering selected amino acid residues can help overcome the cross-species entry barrier, which, in turn, facilitates replication and adaptation of the virus in a new host species.

Our findings suggest that downstream, open Env conformations facilitate usage of rhCD4 and highlight that most T/F and early-stage HIV-1 Envs have an inherently low propensity to use rhCD4. For instance, only one (subtype D Env 191859) of the eight early-stage Envs tested was able to use physiological levels of rhCD4 for viral entry. Testing engineered I423A substitution in 191859 Env resulted in ~2- to 3-fold improvement in usage of physiological levels of rhCD4 for viral entry (Fig. S4), suggesting that opening of the Env improves the efficiency of rhCD4 usage. Taken together, our findings explain why development of SHIVs encoding T/F and early-stage Envs has been challenging and often requires extensive adaptation in human and/or rhesus lymphocytes—a process that typically selects for open Env conformation (2, 10, 20). Consistent with this notion, SHIV-BG505 encoding A204E adaptive mutation, previously identified through *in vitro* evolution experiments (20), displayed the highest replication in rhesus lymphocytes, viral-host membrane fusion, and sensitivity to soluble CD4. These findings also offer an explanation as to why some existing pathogenic SHIVs derived using primary HIV-1 Envs display high sensitivity to soluble CD4 (26–28), which correlates with open Env conformation in which the CD4 binding site is exposed.

In support of our findings that open Env conformations facilitates rhCD4 usage, prior studies have determined the effects of single amino acid substitutions on Env conformational state by measuring sensitivity to broadly neutralizing antibodies (bNAbs) and sCD4. L193A and I423A substitutions in three different Envs representing a T/F (BG505.W6M.C2), an acute-stage clone (ZM53M.PB12), and a chronic-stage isolate (JR-FL) displayed neutralization profiles that are expected for open Env conformations (15, 16). For example, all three

Envs with L193A or I423A substitution were more sensitive to state 2/3-preferring sCD4 and 4E10 bNAb and more resistant to state 1-preferring PG9 and VRC03 bNAbs than the related wild-type Envs. In a separate study, A204E substitution in Env conferred resistance to bNAbs directed to quaternary epitopes and sensitivity to antibodies directed to internal epitopes in the V2/V3 Env domains, suggesting that the A204E Env trimer adopts a more open conformation (10). Consistent with this notion, the T/F BG505 Env is ~40-fold more resistant to sCD4 inhibition than chronic-stage JR-FL Env (15, 16). Moreover, BaL Envs are consider tier 1B Envs, and they are sensitive to several antibodies that recognize internal epitopes, such as 830A and 447-52D (CATNAP [https://www.hiv.lanl.gov/components/sequence/HIV/neutralization/index.html]). Thus, the conformation of BaL Envs is probably more open than the Env conformation of BG505 and JR-FL.

Our study also suggests that additional parameters may contribute to efficient infection of rhCD4-expressing target cells. Notably, both JR-FL and BaL Envs efficiently use rhCD4 for entry but may represent different Env conformational states. Thus, additional factors, such as affinity of binding to the rhCD4 and hCD4 receptors, can play a role in the entry process, as has been previously reported (29). Overall, it is likely that the intrinsic conformational state of each Env trimer defines the ability to infect cells expressing rhCD4 and this ability can be further modified by opening or closing the specific HIV-1 Envs. From the perspective of transmission, it might be favorable for the virus to adopt a more closed Env conformation. This is because most neutralizing and antibody-dependent cellular cytotoxicity antibodies in the patients' sera are directed against open Env conformation, and therefore, T/F viruses are likely under selective pressure to maintain Env in a closed conformation to evade host humoral responses (18, 19, 30, 31).

In summary, our findings have helped identify a key parameter for future design of SHIVs: the conformational state of Env. Considerable efforts are being made to engineer SHIVs that encode circulating HIV-1 Env, utilize rhCD4 for entry, replicate in rhesus macaques without extensive adaptation, and retain as much of the biological characteristics of HIV-1 Envs as possible (32–34). Thus, it will be of interest to identify and define the minimal open conformational state of HIV-1 Env that affords usage of rhCD4 and replication of SHIVs in rhesus macaques with minimal impact on Env trimer structure and antigenic profile. Based on the findings of this study, the following considerations could be useful for SHIV design: (i) selection of circulating HIV-1 Env with high inherent propensity to sample downstream, open conformations and (ii) engineering changes in Env that lower the free energy needed for transition to open conformations without significantly altering its antigenicity.

MATERIALS AND METHODS

Cells, envelope clones, plasmids, and proteins. HEK293T (ATCC CRL-3216), HeLa TZM-bl (35) (NIH AIDS Reagent program catalog no. 8129), and Cf2Th/syn CCR5 (36) (NIH AIDS Reagent Program; catalog no. 4662) cells were cultured in Dulbecco's modified Eagle medium (DMEM; Gibco) supplemented with 10% fetal bovine serum (FBS; Sigma), 2 mM L-glutamine (Gibco), and 1× penicillin-streptomycin (Gibco) (complete DMEM). Cf2Th/syn CCR5 cells, which are engineered to express human CCR5, were further supplemented with 400 μg/mL of Geneticin (Gibco) to maintain CCR5 expression. Immortalized rhesus macaque 221 T lymphocytes (21) were cultured in Iscove's modified Dulbecco's medium (IMDM) supplemented with 10% FBS, 2 mM L-glutamine, 1× penicillin-streptomycin, and 100 U/mL of interleukin-2 (Roche) (complete IMDM). Rhesus macaque peripheral blood mononuclear cells (PBMCs) were isolated from whole blood (Washington National Primate Research Center) from two independent donors using human erythrocyte lysing kit (R&D Systems) and 95% Lymphoprep (Stemcell Technologies) following the manufacturer's protocols.

The following Env clones from early HIV-1 infections were used: BG505.W6M.C2, Q23.17, TRO.11, CAAN5342.A2, Du422.1, ZM53M.PB12, QB857.110I.B3, and 191859. As a control, two Env clones (JR-FL and BaL.01) of chronic HIV-1 strains were used. The following Env clones encoding the L193A, I423A, and A204E mutations were used: BG505.W6M.C2, ZM53M.PB12, and JR-FL.

A β-lactamase (BlaM) gene fused to the N terminus of SIVmac239 Vpr (GenBank accession no. M33262) separated by a six-glycine–one-lysine linker was synthesized as a DNA fragment (Integrated DNA Technologies), digested, and ligated into pcDNA3.1 (Invitrogen) using KpnI and NotI restriction sites to generate the pcDNA3.1-BlaM-SIVmac239 Vpr plasmid. All plasmids generated in this study were verified by Sanger DNA sequencing.

Soluble rhCD4 (Met1-Trp390; catalog no. 90274-C08H) and huCD4 (Met 1-Trp 390; catalog no. 10400-H08H) proteins with C-terminal 6×His tags were purchased from Sino Biological.

Pseudovirus and SHIV production. Green fluorescent protein (GFP) reporter pseudoviruses were generated as described previously (37). Briefly, HEK293T cells were cotransfected with 4 μg of Env-deficient HIV-1 proviral plasmid (Q23ΔEnvGFP) and 2 μg of the HIV-1 Env clone of interest using Fugene 6 transfection reagent (Roche) following the manufacturer's protocol. Replication-competent SHIV stocks were generated as described previously (38). The viral titer of each pseudovirus and SHIV stock was determined by infecting TZM-bl cells and staining for β-galactosidase activity 48 h postinfection (35).

Generation of stable cell lines. Cf2Th/syn CCR5 cells stably expressing rhCD4 were generated using methods described previously (39). Briefly, retroviral pseudoviruses were generated in HEK293T cells by cotransfecting pLPCX-rhCD4 (retroviral vector encoding rhCD4), pJK3 (murine leukemia virus [MLV]-based packaging plasmid), and pMD.G (vesicular stomatitis virus glycoprotein [VSV-G] plasmid) at a ratio of 1:1:0.5 using Fugene 6 transfection reagent following the manufacturer's protocol. Forty-eight hours posttransfection, the pseudoviruses were concentrated and used to transduce 10^5 Cf2Th/syn CCR5 cells. Transduced cells were cultured in complete DMEM supplemented with 400 μg/mL of Geneticin (to maintain CCR5 expression) and 2 μg/mL of puromycin (to select for CD4 expression; Sigma). The drug-selected cells with low (rhCD4$_{LOW}$) or high (rhCD4$_{HIGH}$) levels of rhCD4 expression were obtained by sorting the cells on a FACSAria II cell sorter (BD Biosciences) using an allophycocyanin (APC)-conjugated CD4 monoclonal antibody (BD Biosciences; catalog no. 551980) using a previously described CD4 staining method (17). The rhCD4$_{LOW}$ cells were sorted by gating on the CD4-expressing cell population that overlapped with the CD4-stained rhesus macaque PBMCs. The rhCD4$_{HIGH}$ cells were sorted by gating on the top 20% of the CD4-expressing cell population. Cf2Th/syn CCR5 cells stably expressing huCD4 have been described previously (39).

CD4 infectivity assay. Infection of Cf2Th/syn CCR5 cells expressing huCD4, rhCD4$_{LOW}$, and rhCD4$_{HIGH}$ with GFP reporter pseudoviruses was performed as described previously (39). Briefly, cells were infected at multiplicities of infection (MOIs) of 0.1, 0.25, and 1 in the presence of 10 μg/mL of DEAE-dextran by spinoculation at 1,200 × g for 90 min. After 48 h, cells were harvested, fixed in 2% paraformaldehyde, washed twice, and resuspended in fluorescence-activated cell sorter (FACS) buffer (1× phosphate-buffered saline [PBS], 1% FBS, 1 mM EDTA). Cells were analyzed for GFP expression on an Attune NxT flow cytometer (Life Technologies). The data from ~10^4 cells were analyzed using FlowJo version 10.7.1.

Construction of SHIV proviral clones. Full-length proviral SHIV plasmid encoding BG505.W6M.B1 Env (40) with the A204E mutation (SHIV-BG505 A204E) has been described previously (41). The EcoRV-MfeI region of BG505.W6M.B1 Env (wild type [WT]) and its L193A and I423A variants were synthesized as DNA fragments (Twist Biosciences). SHIV-BG505 WT, SHIV-BG505 L193A, and SHIV-BGB505 I423A proviral clones were generated by digesting and ligating the DNA fragments into the SHIV-BG505 A204E proviral plasmid using EcoRV and MfeI restriction sites. The generated SHIV proviral plasmids were verified by DNA sequencing.

SHIV replication time course. Replication of SHIVs was assessed as described previously (38). Briefly, 4 × 10^6 221 T lymphocytes were infected at an MOI of 0.02 by spinoculation at 1,200 × g for 90 min at room temperature. After spinoculation, cells were washed four times with 1 mL of complete IMDM, resuspended in 5 mL of complete IMDM, and plated in one well of a six-well plate. Every 3 days, two-thirds of the cultures was harvested and replenished with fresh, complete IMDM. Viral supernatants were collected from the harvested cultures by pelleting at 650 × g for 5 min at room temperature. Reverse transcriptase (RT) activity in viral supernatants was measured using the RT activity assay.

SHIV neutralization assay. Neutralization of SHIVs with rhCD4 and huCD4 were performed as described previously (16) but using TZM-bl target cells. The calculated half-maximal inhibitory concentration (IC$_{50}$) values represent the soluble CD4 micromolar concentration at which 50% of the virus was neutralized.

CD4-SHIV binding assay. Affinity pulldown assays were performed using Ni Sepharose 6 Fast Flow resin (Cytiva Lifesciences), His-tagged rhCD4 or huCD4, and SHIV stocks to assess binding of CD4 to SHIVs. Twenty microliters of Ni resin was equilibrated in binding buffer (50 mM HEPES [pH 7.5], 250 mM NaCl, 50 mM imidazole, and 2 mM β-mercaptoethanol) by washing three times (10,000 × g for 1 min) with 100 μL of binding buffer. Equilibrated Ni resin was incubated for 10 min with 1 μg of His-CD4 in 20 μL of binding buffer. Binding reactions were set up by adding equal amounts of indicated SHIV virions (equivalent to 800 and 400 mU of RT) in 160 μL of binding buffer and incubated for 1 h at room temperature, under rotation. Reaction mixtures were then washed three times (10,000 × g for 1 min) with 100 μL of binding buffer to remove unbound CD4/virions. The resulting CD4-virion complexes bound to the Ni resin were extracted using 4× Laemmli sample buffer (Bio-Rad), heated at 95°C for 5 min, and subjected to SDS-PAGE/Western blotting. Standard Western blotting procedures were used with the following antibodies: HIV-1 gp120 (NIH AIDS Reagent Program; catalog no. 288) and 6×His tag (Thermo Fisher; catalog no. MA1-21315-HRP).

SHIV fusion assay. The HIV-1 BlaM-Vpr virus fusion assay described previously (42, 43) was modified to evaluate SHIV fusion. Briefly, BlaM-Vpr was modified by swapping the HIV-1 Vpr with the SIVmac239 Vpr to retain the cognate Gag p6-SIVmac Vpr interaction necessary for efficient virion incorporation of Vpr (44). SHIVs containing BlaM-SIVmac239 Vpr fusion protein were generated by cotransfecting HEK293T cells with 4.5 μg of proviral SHIV plasmid and 1.5 μg of pcDNA3.1-BlaM-SIVmac239 Vpr plasmid using Fugene 6 transfection reagent following the manufacturer's protocol. Forty-eight hours posttransfection, virus-containing supernatant was harvested, passed through a 0.2-μm sterile filter, concentrated ~10-fold using Amicon Ultracel 100-kDa filters (Millipore), aliquoted, and stored at −80°C. RT activity of viral stocks was measured using the RT activity assay. A total of 10^5 221 T lymphocytes in

100 μL of complete IMDM were infected with BlaM-SIVmac239 Vpr-containing SHIVs equivalent to 720 mU of RT by spinoculation at 1,200 × g for 90 min, followed by incubation at 37°C and 5% CO_2 for 1 h. Fusion-mediated SHIV entry was quantified by monitoring the conversion of fluorescent BlaM CCF2-AM substrate dye. After infection, cells were washed once with 300 μL of cold CO_2-independent medium (Gibco) without FBS and resuspended in 100 μL of CO_2-independent medium supplemented with 10% FBS. Cells were incubated with CCF2-AM substrate (LiveBLAzer CCF2-AM kit; Invitrogen) following the manufacturer's protocol in the presence of 1.8 mM probenecid (Sigma) for 2 h. Cells were washed three times with 300 μL of cold CO_2-independent medium without FBS and once with 1× PBS, fixed with 200 μL of 2% paraformaldehyde, washed once with 1× PBS, and resuspended in 400 μL of FACS buffer. The fluorescence of cleaved CCF2-AM substrate was measured on an Attune NxT flow cytometer and data were analyzed using FlowJo version 10.7.1.

Reverse transcriptase activity assay. RT activity assay was performed as described previously (43, 45), with minor modifications. Briefly, 5 μL of viral supernatant, viral stock, or RT standard was lysed in 5 μL of 2× lysis buffer (100 mM Tris HCl [pH 7.4], 50 mM KCl, 0.25% Triton X-100, 40% glycerol) in the presence of 4 U of RNaseOUT (Invitrogen) for 10 min at room temperature. Viral lysate was diluted 1:10 by adding 90 μL of nuclease-free water (Life Technologies). Reverse transcriptase quantitative PCRs (qRT-PCRs) were prepared by mixing 9.6 μL of diluted viral lysate with 10.4 μL of reaction mixture containing 10 μL of 2× Maxima SYBR green/ROX qPCR master mix (Thermo Fisher), 0.1 μL of 4-U/μL RNaseOUT, 0.1 μL of 0.8-μg/μL MS2 RNA template (Roche), and 0.1 μL each of 100 μM forward (5'-TCCTGCTCAACTTCCTGTCGAG-3') and reverse (5'-CACAGGTCAAACCTCCTAGGAATG-3') primers. qRT-PCR was performed using a QuantStudio 3 real-time PCR machine (Applied Biosystems). Viral titers were calculated from a standard curve generated using recombinant reverse transcriptase (Millipore; catalog no. 382129).

SUPPLEMENTAL MATERIAL

Supplemental material is available online only.
FIG S1, TIF file, 0.5 MB.
FIG S2, TIF file, 0.2 MB.
FIG S3, TIF file, 0.4 MB.
FIG S4, TIF file, 0.2 MB.

ACKNOWLEDGMENTS

REFERENCES

1. Hatziioannou T, Evans DT. 2012. Animal models for HIV/AIDS research. Nat Rev Microbiol 10:852–867. https://doi.org/10.1038/nrmicro2911.

2. Sharma A, Boyd DF, Overbaugh J. 2015. Development of SHIVs with circulating, transmitted HIV-1 variants. J Med Primatol 44:296–300. https://doi.org/10.1111/jmp.12179.

3. Chen Z, Huang Y, Zhao X, Skulsky E, Lin D, Ip J, Gettie A, Ho DD. 2000. Enhanced infectivity of an R5-tropic simian/human immunodeficiency virus carrying human immunodeficiency virus type 1 subtype C envelope after serial passages in pig-tailed macaques (Macaca nemestrina). J Virol 74:6501–6510. https://doi.org/10.1128/jvi.74.14.6501-6510.2000.

4. Harouse JM, Gettie A, Eshetu T, Tan RC, Bohm R, Blanchard J, Baskin G, Cheng-Mayer C. 2001. Mucosal transmission and induction of simian AIDS by CCR5-specific simian/human immunodeficiency virus SHIV(SF162P3). J Virol 75:1990–1995. https://doi.org/10.1128/JVI.75.4.1990-1995.2001.

5. Ndung'u T, Lu Y, Renjifo B, Touzjian N, Kushner N, Pena-Cruz V, Novitsky VA, Lee TH, Essex M. 2001. Infectious simian/human immunodeficiency virus with human immunodeficiency virus type 1 subtype C from an African isolate: rhesus macaque model. J Virol 75:11417–11425. https://doi.org/10.1128/JVI.75.23.11417-11425.2001.

6. Nishimura Y, Shingai M, Willey R, Sadjadpour R, Lee WR, Brown CR, Brenchley JM, Buckler-White A, Petros R, Eckhaus M, Hoffman V, Igarashi T, Martin MA. 2010. Generation of the pathogenic R5-tropic simian/human immunodeficiency virus SHIVAD8 by serial passaging in rhesus macaques. J Virol 84:4769–4781. https://doi.org/10.1128/JVI.02279-09.

7. Pal R, Taylor B, Foulke JS, Woodward R, Merges M, Praschunus R, Gibson A, Reitz M. 2003. Characterization of a simian human immunodeficiency virus encoding the envelope gene from the CCR5-tropic HIV-1 Ba-L. J Acquir Immune Defic Syndr 33:300–307. https://doi.org/10.1097/00126334-200307010-00003.

8. Song RJ, Chenine AL, Rasmussen RA, Ruprecht CR, Mirshahidi S, Grisson RD, Xu W, Whitney JB, Goins LM, Ong H, Li PL, Shai-Kobiler E, Wang T, McCann CM, Zhang H, Wood C, Kankasa C, Secor WE, McClure HM, Strobert E, Else JG, Ruprecht RM. 2006. Molecularly cloned SHIV-1157ipd3N4: a highly replication-competent, mucosally transmissible R5 simian-human immunodeficiency virus encoding HIV clade C Env. J Virol 80:8729–8738. https://doi.org/10.1128/JVI.00558-06.

9. Sharma A, Overbaugh J. 2018. CD4-HIV-1 envelope interactions: critical insights for the simian/HIV/macaque model. AIDS Res Hum Retroviruses 34:778–779. https://doi.org/10.1089/AID.2018.0110.

10. Boyd DF, Peterson D, Haggarty BS, Jordan AP, Hogan MJ, Goo L, Hoxie JA, Overbaugh J. 2015. Mutations in HIV-1 envelope that enhance entry with the macaque CD4 receptor alter antibody recognition by disrupting quaternary interactions within the trimer. J Virol 89:894–907. https://doi.org/10.1128/JVI.02680-14.

11. Munro JB, Gorman J, Ma X, Zhou Z, Arthos J, Burton DR, Koff WC, Courter JR, Smith AB, III, Kwong PD, Blanchard SC, Mothes W. 2014. Conformational dynamics of single HIV-1 envelope trimers on the surface of native virions. Science 346:759–763. https://doi.org/10.1126/science.1254426.

12. Ma X, Lu M, Gorman J, Terry DS, Hong X, Zhou Z, Zhao H, Altman RB, Arthos J, Blanchard SC, Kwong PD, Munro JB, Mothes W. 2018. HIV-1 Env trimer opens through an asymmetric intermediate in which individual protomers adopt distinct conformations. Elife 7:e34271. https://doi.org/10.7554/eLife.34271.

13. Wang Q, Finzi A, Sodroski J. 2020. The conformational states of the HIV-1 envelope glycoproteins. Trends Microbiol 28:655–667. https://doi.org/10.1016/j.tim.2020.03.007.

14. Kwon YD, Finzi A, Wu X, Dogo-Isonagie C, Lee LK, Moore LR, Schmidt SD, Stuckey J, Yang Y, Zhou T, Zhu J, Vicic DA, Debnath AK, Shapiro L, Bewley CA, Mascola JR, Sodroski JG, Kwong PD. 2012. Unliganded HIV-1 gp120 core structures assume the CD4-bound conformation with regulation by quaternary interactions and variable loops. Proc Natl Acad Sci U S A 109: 5663–5668. https://doi.org/10.1073/pnas.1112391109.

15. Herschhorn A, Gu C, Moraca F, Ma X, Farrell M, Smith AB, III, Pancera M, Kwong PD, Schon A, Freire E, Abrams C, Blanchard SC, Mothes W, Sodroski JG. 2017. The beta20-beta21 of gp120 is a regulatory switch for HIV-1 Env conformational transitions. Nat Commun 8:1049. https://doi.org/10.1038/s41467-017-01119-w.

16. Herschhorn A, Ma X, Gu C, Ventura JD, Castillo-Menendez L, Melillo B, Terry DS, Smith AB, III, Blanchard SC, Munro JB, Mothes W, Finzi A, Sodroski J. 2016. Release of gp120 restraints leads to an entry-competent intermediate state of the HIV-1 envelope glycoproteins. mBio 7:e01598-16. https://doi.org/10.1128/mBio.01598-16.

17. Humes D, Emery S, Laws E, Overbaugh J. 2012. A species-specific amino acid difference in the macaque CD4 receptor restricts replication by global circulating HIV-1 variants representing viruses from recent infection. J Virol 86:12472–12483. https://doi.org/10.1128/JVI.02176-12.

18. Keele BF, Giorgi EE, Salazar-Gonzalez JF, Decker JM, Pham KT, Salazar MG, Sun C, Grayson T, Wang S, Li H, Wei X, Jiang C, Kirchherr JL, Gao F, Anderson JA, Ping LH, Swanstrom R, Tomaras GD, Blattner WA, Goepfert PA, Kilby JM, Saag MS, Delwart EL, Busch MP, Cohen MS, Montefiori DC, Haynes BF, Gaschen B, Athreya GS, Lee HY, Wood N, Seoighe C, Perelson AS, Bhattacharya T, Korber BT, Hahn BH, Shaw GM. 2008. Identification and characterization of transmitted and early founder virus envelopes in primary HIV-1 infection. Proc Natl Acad Sci U S A 105:7552–7557. https://doi.org/10.1073/pnas.0802203105.

19. Han Q, Jones JA, Nicely NI, Reed RK, Shen X, Mansouri K, Louder M, Trama AM, Alam SM, Edwards RJ, Bonsignori M, Tomaras GD, Korber B, Montefiori DC, Mascola JR, Seaman MS, Haynes BF, Saunders KO. 2019. Difficult-to-neutralize global HIV-1 isolates are neutralized by antibodies targeting open envelope conformations. Nat Commun 10:2898. https://doi.org/10.1038/s41467-019-10899-2.

20. Humes D, Overbaugh J. 2011. Adaptation of subtype A human immunodeficiency virus type 1 envelope to pig-tailed macaque cells. J Virol 85: 4409–4420. https://doi.org/10.1128/JVI.02244-10.

21. Alexander L, Du Z, Rosenzweig M, Jung JU, Desrosiers RC. 1997. A role for natural simian immunodeficiency virus and human immunodeficiency virus type 1 nef alleles in lymphocyte activation. J Virol 71:6094–6099. https://doi.org/10.1128/JVI.71.8.6094-6099.1997.

22. Finzi A, Xiang SH, Pacheco B, Wang L, Haight J, Kassa A, Danek B, Pancera M, Kwong PD, Sodroski J. 2010. Topological layers in the HIV-1 gp120 inner domain regulate gp41 interaction and CD4-triggered conformational transitions. Mol Cell 37:656–667. https://doi.org/10.1016/j.molcel.2010.02.012.

23. Haim H, Strack B, Kassa A, Madani N, Wang L, Courter JR, Princiotto A, McGee K, Pacheco B, Seaman MS, Smith AB, III, Sodroski J. 2011. Contribution of intrinsic reactivity of the HIV-1 envelope glycoproteins to CD4-independent infection and global inhibitor sensitivity. PLoS Pathog 7: e1002101. https://doi.org/10.1371/journal.ppat.1002101.

24. Kassa A, Madani N, Schon A, Haim H, Finzi A, Xiang SH, Wang L, Princiotto A, Pancera M, Courter J, Smith AB, III, Freire E, Kwong PD, Sodroski J. 2009. Transitions to and from the CD4-bound conformation are modulated by a single-residue change in the human immunodeficiency virus type 1 gp120 inner domain. J Virol 83:8364–8378. https://doi.org/10.1128/JVI.00594-09.

25. Xiang SH, Kwong PD, Gupta R, Rizzuto CD, Casper DJ, Wyatt R, Wang L, Hendrickson WA, Doyle ML, Sodroski J. 2002. Mutagenic stabilization and/or disruption of a CD4-bound state reveals distinct conformations of the human immunodeficiency virus type 1 envelope glycoprotein. J Virol 76:9888–9899. https://doi.org/10.1128/jvi.76.19.9888-9899.2002.

26. Joag SV, Li Z, Foresman L, Stephens EB, Zhao LJ, Adany I, Pinson DM, McClure HM, Narayan O. 1996. Chimeric simian/human immunodeficiency virus that causes progressive loss of CD4+ T cells and AIDS in pig-tailed macaques. J Virol 70:3189–3197. https://doi.org/10.1128/JVI.70.5.3189-3197.1996.

27. Tan RC, Harouse JM, Gettie A, Cheng-Mayer C. 1999. In vivo adaptation of SHIV (SF162): chimeric virus expressing a NSI, CCR5-specific envelope protein. J Med Primatol 28:164–168. https://doi.org/10.1111/j.1600-0684.1999.tb00265.x.

28. Ren W, Mumbauer A, Gettie A, Seaman MS, Russell-Lodrigue K, Blanchard J, Westmoreland S, Cheng-Mayer C. 2013. Generation of lineage-related, mucosally transmissible subtype C R5 simian-human immunodeficiency viruses capable of AIDS development, induction of neurological disease, and coreceptor switching in rhesus macaques. J Virol 87:6137–6149. https://doi.org/10.1128/JVI.00178-13.

29. Warren CJ, Meyerson NR, Dirasantha O, Feldman ER, Wilkerson GK, Sawyer SL. 2019. Selective use of primate CD4 receptors by HIV-1. PLoS Biol 17:e3000304. https://doi.org/10.1371/journal.pbio.3000304.

30. Richman DD, Wrin T, Little SJ, Petropoulos CJ. 2003. Rapid evolution of the neutralizing antibody response to HIV type 1 infection. Proc Natl Acad Sci U S A 100:4144–4149. https://doi.org/10.1073/pnas.0630530100.

31. Prevost J, Richard J, Ding S, Pacheco B, Charlebois R, Hahn BH, Kaufmann DE, Finzi A. 2018. Envelope glycoproteins sampling states 2/3 are susceptible to ADCC by sera from HIV-1-infected individuals. Virology 515: 38–45. https://doi.org/10.1016/j.virol.2017.12.002.

32. Li H, Wang S, Kong R, Ding W, Lee FH, Parker Z, Kim E, Learn GH, Hahn P, Policicchio B, Brocca-Cofano E, Deleage C, Hao X, Chuang GY, Gorman J, Gardner M, Lewis MG, Hatziioannou T, Santra S, Apetrei C, Pandrea I, Alam SM, Liao HX, Shen X, Tomaras GD, Farzan M, Chertova E, Keele BF, Estes JD, Lifson JD, Doms RW, Montefiori DC, Haynes BF, Sodroski JG, Kwong PD, Hahn BH, Shaw GM. 2016. Envelope residue 375 substitutions in simian-human immunodeficiency viruses enhance CD4 binding and replication in rhesus macaques. Proc Natl Acad Sci U S A 113: E3413–E3422. https://doi.org/10.1073/pnas.1606636113.

33. Del Prete GQ, Ailers B, Moldt B, Keele BF, Estes JD, Rodriguez A, Sampias M, Oswald K, Fast R, Trubey CM, Chertova E, Smedley J, LaBranche CC, Montefiori DC, Burton DR, Shaw GM, Markowitz M, Piatak M, Jr, KewalRamani VN, Bieniasz PD, Lifson JD, Hatziioannou T. 2014. Selection of unadapted, pathogenic SHIVs encoding newly transmitted HIV-1 envelope proteins. Cell Host Microbe 16:412–418. https://doi.org/10.1016/j.chom.2014.08.003.

34. Chang HW, Tartaglia LJ, Whitney JB, Lim SY, Sanisetty S, Lavine CL, Seaman MS, Rademeyer C, Williamson C, Ellingson-Strouss K, Stamatatos L, Kublin J, Barouch DH. 2015. Generation and evaluation of clade C simian-human immunodeficiency virus challenge stocks. J Virol 89:1965–1974. https://doi.org/10.1128/JVI.03279-14.

35. Wei X, Decker JM, Liu H, Zhang Z, Arani RB, Kilby JM, Saag MS, Wu X, Shaw GM, Kappes JC. 2002. Emergence of resistant human immunodeficiency virus type 1 in patients receiving fusion inhibitor (T-20) monotherapy. Antimicrob Agents Chemother 46:1896–1905. https://doi.org/10.1128/AAC.46.6.1896-1905.2002.

36. Farzan M, Mirzabekov T, Kolchinsky P, Wyatt R, Cayabyab M, Gerard NP, Gerard C, Sodroski J, Choe H. 1999. Tyrosine sulfation of the amino terminus of CCR5 facilitates HIV-1 entry. Cell 96:667–676. https://doi.org/10.1016/s0092-8674(00)80577-2.

37. Nahabedian J, Sharma A, Kaczmarek ME, Wilkerson GK, Sawyer SL, Overbaugh J. 2017. Owl monkey CCR5 reveals synergism between CD4 and CCR5 in HIV-1 entry. Virology 512:180–186. https://doi.org/10.1016/j.virol.2017.09.018.

38. Sharma A, McLaughlin RN, Jr, Basom RS, Kikawa C, OhAinle M, Yount JS, Emerman M, Overbaugh J. 2019. Macaque interferon-induced transmembrane proteins limit replication of SHIV strains in an envelope-dependent

manner. PLoS Pathog 15:e1007925. https://doi.org/10.1371/journal.ppat
.1007925.

39. Meyerson NR, Sharma A, Wilkerson GK, Overbaugh J, Sawyer SL. 2015. Identi-
fication of owl monkey CD4 receptors broadly compatible with early-stage
HIV-1 isolates. J Virol 89:8611–8622. https://doi.org/10.1128/JVI.00890-15.

40. Wu X, Parast AB, Richardson BA, Nduati R, John-Stewart G, Mbori-Ngacha D,
Rainwater SM, Overbaugh J. 2006. Neutralization escape variants of human
immunodeficiency virus type 1 are transmitted from mother to infant. J Virol
80:835–844. https://doi.org/10.1128/JVI.80.2.835-844.2006.

41. Boyd DF, Sharma A, Humes D, Cheng-Mayer C, Overbaugh J. 2016. Adapting
SHIVs in vivo selects for envelope-mediated interferon-alpha resistance. PLoS
Pathog 12:e1005727. https://doi.org/10.1371/journal.ppat.1005727.

42. Cavrois M, De Noronha C, Greene WC. 2002. A sensitive and specific
enzyme-based assay detecting HIV-1 virion fusion in primary T lympho-
cytes. Nat Biotechnol 20:1151–1154. https://doi.org/10.1038/nbt745.

43. Roesch F, OhAinle M, Emerman M. 2018. A CRISPR screen for factors
regulating SAMHD1 degradation identifies IFITMs as potent inhibitors
of lentiviral particle delivery. Retrovirology 15:26. https://doi.org/10
.1186/s12977-018-0409-2.

44. Selig L, Pages JC, Tanchou V, Preveral S, Berlioz-Torrent C, Liu LX,
Erdtmann L, Darlix J, Benarous R, Benichou S. 1999. Interaction with
the p6 domain of the gag precursor mediates incorporation into vi-
rions of Vpr and Vpx proteins from primate lentiviruses. J Virol 73:
592–600. https://doi.org/10.1128/JVI.73.1.592-600.1999.

45. Vermeire J, Naessens E, Vanderstraeten H, Landi A, Iannucci V, Van Nuffel
A, Taghon T, Pizzato M, Verhasselt B. 2012. Quantification of reverse tran-
scriptase activity by real-time PCR as a fast and accurate method for titra-
tion of HIV, lenti- and retroviral vectors. PLoS One 7:e50859. https://doi
.org/10.1371/journal.pone.0050859.